Mausam, (1991), **42**, 4, 339-346

551.553.11 : 551.511.61

Numerical simulation of sea breeze in south Andamans

S. C. KAR and N. RAMANATHAN

Centre for Atmospheric Sciences, I. I. T., New Delhi

(Received 13 September 1990)

सार — त्रिविमा संख्यात्मक मध्य मापक्रम निदर्श के प्रयोग से दक्षिण अंडमान द्वीप में वायु प्रवाह का अनुकार किया गया है। पोर्ट ब्लेयर के प्रेक्षण प्रारंभिक आंकड़ों के रूप में प्रयुक्त किए गए हैं। सतह पर्वत विज्ञान, मृदा आर्द्रता, मृदा एलबिडो विविधताएं और वनस्पति प्रभाव निदर्श में सम्मिलित हैं। इन कारकों के समुद्र/भूमि संचरण पर मिश्रित प्रभाव परिमाणात्मकरूप से प्राप्त किया गया है। निदर्श अनुकार परिणामों की तुलना उपलब्ध प्रेक्षणों से की गई है। प्राप्त किए गए मुख्य परिणाम हैं: (1) द्वीप की विभेदक उष्णता से प्रभावित मध्य मापक्रम संचरण स्थलाकृति द्वारा तीव्र हो गए। (2) भूमि वनस्पति आवरण वायुमंडल के लिए उच्च मात्रा में प्रक्षुब्ध उष्मा अभिवाहों का वहन करता है और मध्य संचरण उच्च तीव्रता से प्रकट हुए। (3) और, यदि हम अभिवाह (फ्लक्स) की पार्श्व विविधताओं को स्थलाकृतिक और तटीय असमतियों के साथ सम्मिलित करें तो प्रभावित मध्य मापक्रम संचरण, अनुरेखांश दिशा के साथ भिन्न तीव्रता के साथ प्रकट हुए तथा थलीय वेधन दूरी वाई (y) दिशा में परिवर्तित हुई। समुद्री समीर का अधिकतम थलीय वेधन वहां देखा गया जहां कि भूमि चौड़ी थी और भूभाग की ऊंचाई अधिकतम थी। शक्तिशाली समुद्र समीर द्वीप के केन्द्रीय/उत्तरी भागों में अनुकरित हुआ।

ABSTRACT. The air flow over the south Andaman island is simulated using a three dimensional numerical meso-scale model. Port Blair observations are used as initial data. The surface orography, soil moisture, soil albedo variations and vegetation effects are included in the model. The combined effect of these factors on the development of sea/land breeze circulations is obtained quantitatively. The model simulated results are compared with the available observations. The principal results obtained are : (1) The meso-scale circulations induced by the differential heating of the island were intensified by topography. (2) The ground vegetative cover transport higher amount of turbulent heat fluxes to the atmosphere and the meso-circulations appeared with higher intensities. (3) If we include the lateral variations of flux with topographic and coastal asymmetries the induced meso-scale circulations appeared with different intensities along meridional direction and the inland penetration distances varied in y direction. The maximum inland penetration of sea breeze was seen, where the inland was widest and terrain height was maximum. Stronger sea breeze was simulated over the central/northern parts of the island.

Key words — Sea breeze, Trubulent heat flux, Albedo, Thermal stability, Soil moisture, Vegetation.

1. Introduction

Observational studies indicate that weather is often induced by heated islands. Analytical and numerical studies have been undertaken to study the impact of islands on the synoptic flow. Although several islands are present in Indian Ocean, little attention has been paid to their contribution to weather changes. The properties of induced disturbances are governed by the size, shape, topography and orientation of the islands to the prevailing wind and atmospheric stability.

The above reasons have encouraged us to undertake a two-dimensional (2D) study over the Andaman islands (Kar and Ramanathan 1987). These islands were chosen because of (*i*) simple topographical features and (*ii*) proximity to an area of cyclogenesis.

In many atmospheric prediction models the nature of the ground surface, such as the ground albedo and soil moisture variations during the simulated period are ignored. The importance of soil moisture variations has been emphasised by several investigators (Deardorff 1978, Mccumber and Pielke 1981).

Similarly, the contribution of diabatic turbulent heat fluxes to the atmosphere by ground vegetation is usually neglected. The vegetation acts as a secondary source of emission by thermal radiation. Deardorff (1978), Mccumber (1980), Yamada (1982), Garrett (1983) have shown that boundary layer circulations are substantially modified by the presence of vegetation.

As the atmospheric flows are three dimensional (3D), the neglect of lateral variations of atmospheric parameters and terrain asymmetries are physically unrealistic. This aspect was brought out in earlier studies (Neumann and Mahrer, 1974; Mahrer and Pielke, 1976; Ookouchi and Wakata 1984, Abbs 1986). Thus a 3D simulation study is more appropriate because it brings out atmospheric flow features that are not resolved by a two-dimensional model.

The object of the present study is to estimate the intensity of meso-scale flows under the combined effect of above factors and to determine their significance on the flow pattern.

2. General characteristics of the region

The Andaman island chain (10-14°N, 92-94°E) in the Bay of Bengal has an average width of 25 km. Most of the terrain has an elevation less than 200 m with a few peaks above 300 m. The principal soil is loamy sand. Bamboo and teak wood forests cover nearly 86% of the total area. The island chain receives annual rainfall of about 300 cm. A 30 years climatological record shows that for April (selected month of our simulation) the diurnal variation of temperature is 6°C. The average relative humidity is 70%. The mean wind speed is 8.7 kmph and the mean wind direction is northeasterly. The average cloud cover is about 4 oktas.

2.1. *Selected day for simulation*

As little is known about the energy exchange between synoptic and local circulations, data were gathered on days free of large scale synoptic disturbances with no ground precipitation. The 1 April 1969 was found to satisfy the above criteria. Thus, simulations were performed for this day with 0000 GMT Port Blair observations as the initial data. Similar simulations based on a day's data were performed earlier by Nickerson (1979), Segal *et al.* (1982).

3. Model aspects

The model employed in this investigation is a 3 dimensional version of the hydrostatic primitive equation meso-scale model originally developed by Mahrer and Pielke (1977). This model uses a terrain following co-ordinate system. The vertical turbulent exchange coefficients for momentum, heat and moisture are calculated as a function of atmospheric stability using Monin-Obukhov similarity theory. The horizontal exchange coefficient is specified by a low pass filter which also removes 2 grid length waves. The land surface temperature is calculated by a surface energy balance equation which balances the incoming solar radiation with outgoing terrestrial radiation and turbulent heat fluxes. This model remains well documented and often used in several studies as mentioned earlier.

This model is coupled with a soil parameterization scheme developed by Mccumber and Pielke (1981) and a vegetation parameterization scheme developed by Deardorff (1978) and Mccumber (1980) to include the soil moisture, soil albedo variation and vegetation effects. The relevant governing equations of the parameterization schemes are given in chapter 11, Pielke (1984). For brevity, we omit the mathematical details here.

4. Initial and boundary conditions

The initial atmospheric data for the model are the wind velocity, temperature and moisture. These were taken from the synoptic observations recorded at Port Blair. The initial soil moistures profile, soil moisture content (η) were taken from climatological records. The soil and and vegetation characteristics were obtained from Clapp and Hornberger (1978), Lee (1978), Perrier (1978) and

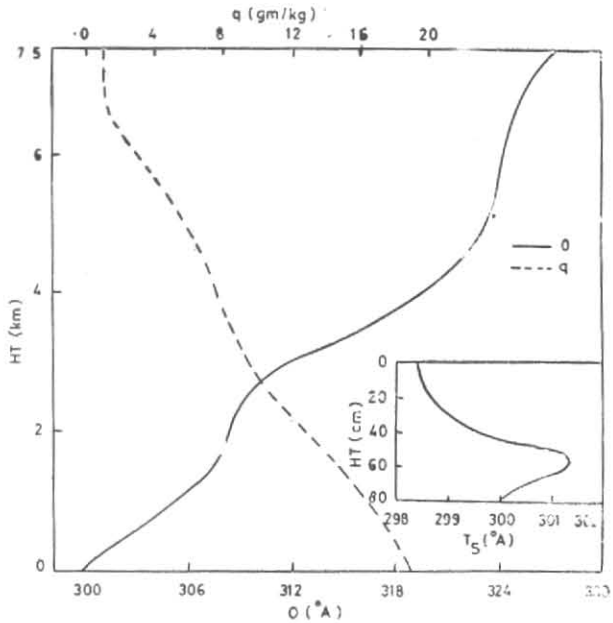

Fig. 1. Profiles of potential temperature (θ), specific humidity (q) and soil temperature (Ts) (inset diagram) (Initial data 1st April 1969). For 3D simulations, all grid points in the entire computational domain were initialized with the same synoptic data given above and in Table 1 (This procedure is commonly followed in data sparse regions)

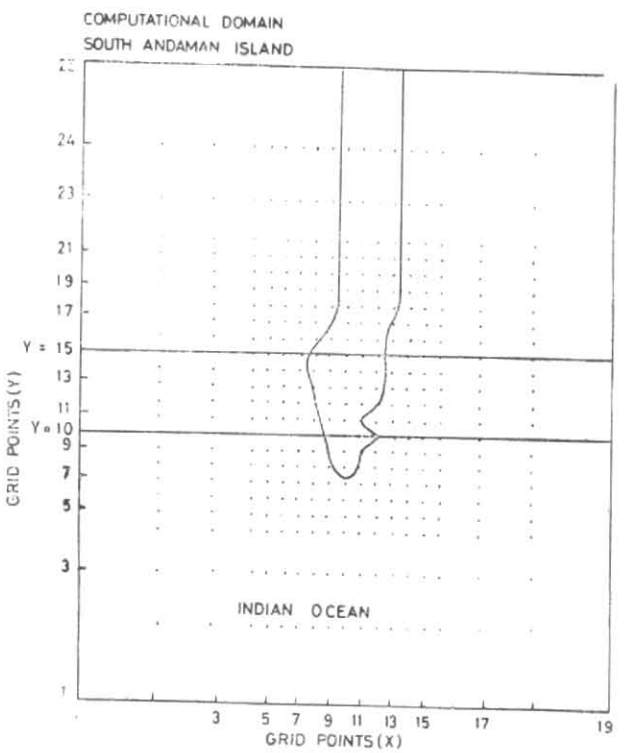

Fig. 2. Computational domain with grid point arrangement. $y=10$ line denotes cross-section for Port Blair $y=15$ line passes through widest part of the island

TABLE 1

Observed wind speed and direction 0000 GMT Port Blair observation 1 April 1959

Height (m)	Speed (m/s)	Direction (°) from north
2	0.0	360
500	1.5	60
1000	1.0	75
1500	2.0	90
2000	6.0	100
2500	6.0	110
3120	6.0	120
3700	4.0	105
4400	4.0	100
5050	7.0	50
6600	8.0	70
7500	9.0	80

Deardorff (1978). The 1 April 1969 synoptic observations for which this detailed 3D-study was performed are given in Table 1 and Fig. 1. These remain identical as in our earlier study (Kar and Ramanathan 1987). The large scale surface pressure and temperature were taken to be 1013 mb and 300° K respectively as observed. The terrain heights, evaluated from a survey of India map, were smoothed using a 9-point smoother. Within the PBL winds were determined by assuming a balance of shear stress, the coriolis and the pressure gradient forces. Above the PBL the model was initialized with observed synoptic data. The top and bottom boundary conditions over bare ground and with vegetation cover were taken to be the same as detailed in our earlier study (1989). Zero gradient boundary conditions were taken for the flow variables at the model lateral boundaries.

4.1. *Computational domain*

A rectangular area with 192km × 238 km in the x and y directions covering the south Andaman island was chosen for the study. With the specified initial and boundary conditions as described in the previous section, the governing equations were integrated with a grid mesh of $19 \times 25 \times 12$ (x, y and z), using a time step of 45 sec., starting from local sun rise time. Better resolution at the lateral edges of the island and over the island were obtained using a variable distance grid in x, y and z directions. This also eliminated the lateral and upper boundary effects from the integrated domain. The computational domain with grid point arrangements is shown in Fig. 2. The lines $y=10$ and $y=15$ drawn across the Fig. 2 passes through Port Blair, situated in the eastern edge of the island at $x=12$, and over the widest cross-section of the island respectively. Over and near the island edges the distance between two grid points ($\triangle x$ and $\triangle y$) was taken to be 6 km. Near the lateral boundaries to avoid the boundary effects $\triangle x$ and $\triangle y$ were increased to 30 km. Also in the vertical a variable distance grid was utilised. These were situated at height 30, 100, 500, 1000, 1500, 2000, 2500, 3120, 3700 5050, 6600, 7500 m respectively. The top of the model was chosen at 7.5 km by trial and error method so that there were no reflections or boundary effects into the region of the computation.

4.2. *Selection of input parameters/data*

The saturated moisture potential, saturated hydraulic conductivity, porosity, volumetric heat capacity of loamy sand, the predominant soil in Andamans, were assigned the following values 9.0 cm, 0.01563 cm/s, 0.41, 0.336 cal $cm^{-1}°C$ respectively from Clapp and Hornberger (1978) studies. The initial soil moisture content (% by vol.) was taken to be 8.5 %, near the field capacity of loamy sand as observed in forested areas (Simpson 1985). The emissivity of the ground for long wave radiation was assumed to be unity.

The temporal variation of the ground surface albedo was calculated as a function of soil moisture using Idso *et al.* (1975) relations.

The emissivity, albedo, surface resistance, leaf area index (LAI) for tropical vegetation were taken as 0.95, 0.15, 1.3 s cm^{-1} and 6 ($=7\sigma f$) respectively from Lee (1978), Perrier (1978), Oke (1978) and Deardorff (1978) studies respectively. The emissivity values range between 0.95 & 0.98 and surface resistance (=stomatal resistance/LAI) between 1.0 & 3.0 s cm^{-1} (Perrier 1978). Both these parameters depend upon the age and physical condition of vegetation etc. Conservative values, as given above, were used in the simultations. The albedo, LAI, variations, if any, are not reported in literature for tropical vegetation.

The surface drag coefficient (C_g) was calculated by Thom's (1971) relation.

$$C_g = \left[\frac{k}{\ln\left(\frac{Z-D}{Z_0}\right)} \right]^{\frac{1}{2}}$$

where, $k = 0.35$, $Z_o = 0.08\, H_c$, $D = 0.76\, H_c$, H_c is average height of the plant canopy and Z is the first grid level of the model (30 m).

For simulation purposes, H_c was taken as 13 metres (40 feet) the averate height of bamboo and teak forest prevalent in Andamans. The drag coefficient (C_{go}) for bare ground was taken to have the value 10^{-3}. The net surface drag coefficient (C_{gN}) was obtained by the weighted average of the bare soil and vegetation using the relation :

$$C_{gN} = 0.86\, C_g + 0.14\, C_{go}$$

The zero-plane displacement height (D) and roughness length (Z_o) were specified from Mccumber (1980) studies using Deardorff suggestions. Both the above parameters depend on the vegetation height and wind speed. Several formulations for these parameters each differing by small amounts such as $D=0.63\ H_c$ (Monteith 1973), $D=2/3\ H_c$ (Oke 1978), $D=0.7\ H_c$ (Stanhill 1969), $D=0.7\ H_c$ (Coinco 1985), $Z_0=0.14\ H_c$ (Coinco 1985), $Zo=H_c \exp(-0.98)$ (Oke 1978), $Z_o=0.174\ H_c + 0.227$ (Jagar 1985) are reported

The chosen values agree with Amazon forest observations (Deabreausa *et al.* 1988). The transfer coefficient (C_f) of the vegetation was calculated using Kumar and Barathakur (1971) relation.

$$C_f = 0.01 \left(1 + \frac{0.3}{u_{af}}\right) ; \; u_{af} = 0.83\, C_g^{\frac{1}{2}}\, u_a$$

u_a is wind speed at first grid level of the model. Simulations were performed only for synoptically clear day with no clouds sighted in the Port Blair observations. Thus, the inclusion of cloud effects in radiation calculations did not arise.

In the absence of any other data other than Port Blair observations in this area, for 3D simulations the entire domain was initialized with Port Blair data after dynamic initialization as described earlier. Similar procedure was followed in Mahrer and Pielke (1976), for Barbados island studies. An average vegetation coverage (σf) 86% of the land area (DST atlas) with leaf area index 7 σf (Deardorff 1978) were used in simulations.

Our sensitivity tests (Kar and Ramanathan 1990) have shown β (Bowen ratio) remains insensitive to the change in leaf area index values during daylight hours. Negative β values were obtained after sunset due to change in thermal stability of the atmosphere and subsequent change in the direction of sensible heat flux.

In the calculations bare soil and vegetation were weighted with the coefficients 0.14 and 0.86 respectively corresponding to 86% vegetation coverage of the land in this area.

5. Results and discussion

The principal factors that govern the intensity and horizontal extent of perturbations are : (*i*) the island topography, (*ii*) geometry of the coast lines, (*iii*) soil moisture, (*iv*) vegetation, (*v*) diurnal variation of surface temperature, and (*vi*) the intensity of the synoptic flow. In this study the initial soil moisture and the synoptic observations were specified as initial data and these were not varied. The diurnal variation of surface temperature was calculated from the surface energy balance equation. Three dimensional (3D) simulations were made for the following cases :

(1) Flat island without vegetation,

(2) Island with topography and without vegetation,

(3) Island with topography and vegetation.

The initial soil moisture content was taken from observations. To consider the changes introduced by the lateral variations of parameters on the developed flow, a 2D simulation with topography and vegetation was also performed and compared with 3D simulation. A summary of model simulated results for $y=10$ cross-section is shown in Table 2.

The simulations were performed from sunrise to next day sunrise (24 hours). The reported are instant values and maximum during the entire simulation period are given in each case. The simulated β (Bowen ratio)

TABLE 2

Particulars	Case 1	Case 2	Case 3	Case 4
Surface temp. (°K) at 1200 hr	312.1	311.1	308.0	309.0
Specific humidity of soil (g/kg) at 1200 hr	31.9	30.8	33.0	32.0
Sensible heat flux (w/m²) at 1200 hr	—	150	275	275
Latent heat flux (w/m²) at 1200 hr	—	350	400	340
Boundary layer depth at 1800 hr	600 m	715 m	1150 m	1900 m
Sea breeze onset/retreat time (IST)	1000/ 1900 hr	900/ 2000 hr	900/ 2000 hr	900/ 2000 hr
Sea breeze wind speed (m/s) at 1400 hr	1.2	1.8	2.3	2.8
Vertical depth (m) at 1200 hr	200	250	350	580
Inland penetration distance (km) at 1200 hr	7	9	4	6
Vertical velocity 20 m above ground at 1400 hr (cm/s) (IST)	1.0	4.0	6.0	15.0
Land breeze				
Onset time hr (IST)	24.00	21.00	20.00	21.00
Vertical depth (m) at 0400 hr	10.0	20.0	30.0	30.0
Maximum wind speed (m/s) at 0400 hr	0.15	1.6	1.9	2.1

≈0.7 (275/400) is in agreement with Amazon forests observations (Deabreausa *et al.* 1988). In our simulations with vegetation the transfer of sensible and latent heat fluxes by the vegetation to the atmosphere were taken into account. Thus considerable differences in temperature/moisture between air and ground due to vegetative cover appeared. The simulated values were found to be in qualitative agreement with Mccumber's (1980) studies. The plant canopy, which behaves as an elevated heat source raises β values. Amazon observations report β varies between 0.05 & 0.85 during daylight hours.

The influence of topography, vegetation and lateral variations of flow with topographic and coastal asymmetries are obtained from the above results.

5.1. *Topography*

A comparison of case 1 with case 2 results shows the influence of surface topography on the induced perturbations. The complex interaction of sea breeze development with slope winds over rough terrain enhanced the intensity of developed perturbations.

(*i*) Topography accelerated the arrival of sea breeze at the west coast of the island by about an hour.

(*ii*) The horizontal inland penetration distance, wind speed and vertical depth of sea breeze developed were higher with topography than developed over flat island. The vertical velocities of induced perturbations and boundary layer depths developed were higher with topography.

(*iii*) Topography also modified the nocturnal airflow over the island. These are shown by the difference in magnitudes of land breeze speeds developed over the

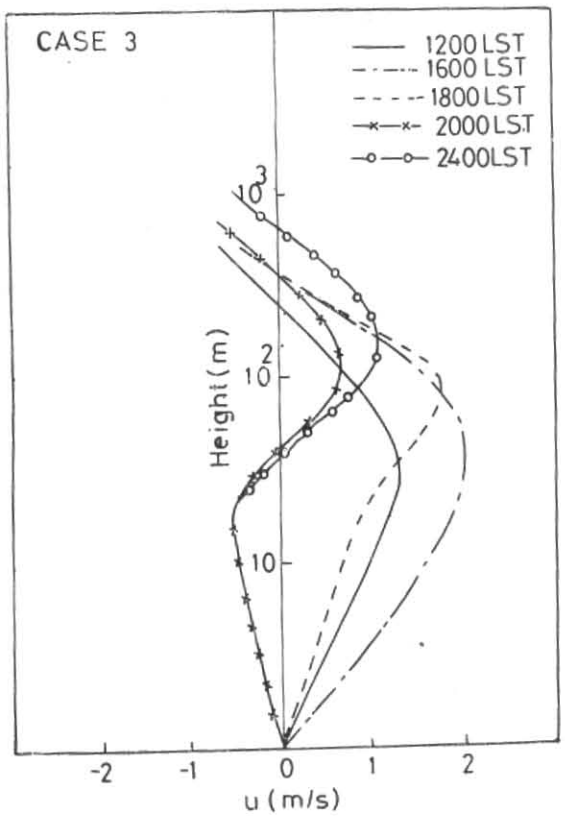

Fig. 3. Sea breeze vertical profiles for case 3 at selected hours

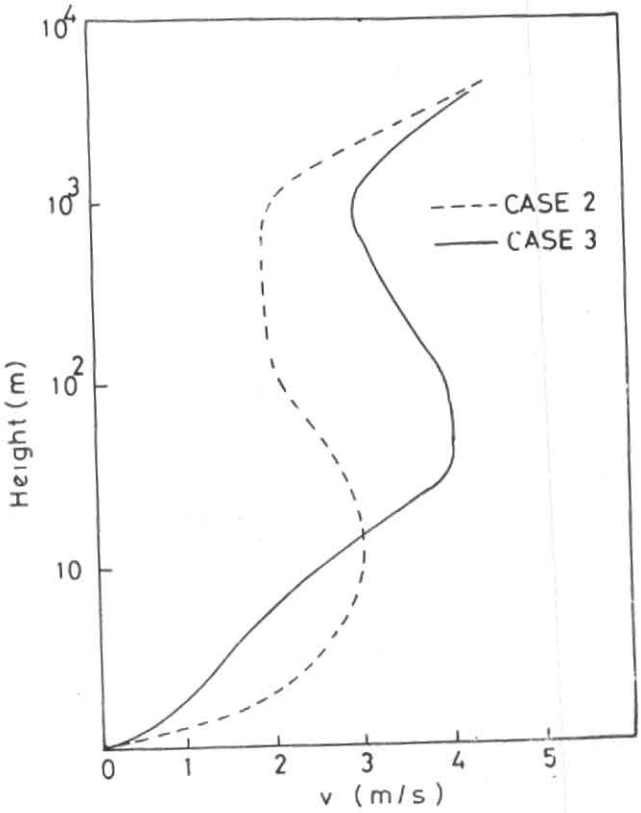

Fig. 4. Horizontal wind speed profiles for case 2 and case 3

island. Due to downslope flows a more intense breeze with a speed of 1.6 m/s was developed with a depth of 30 m over the island with topography.

The corresponding values over flat island were 0.15 m/s and 10 m respectively. The above results show that the topography, in general, intensifies the circulations developed.

5.2. *Vegetation*

The effects due to vegetation canopy are obtained by a comparison of case 2 with case 3 results.

(*i*) With vegetation cover lower surface temperature with higher specific humidity were developed. These were due to shade effects of vegetation on the ground. The diurnal changes of these variables were less than in the case of bare soil. The developed surface temperature, specific humidity and surface albedo were maximum at local noon hours (not shown here).

(*ii*) The calculated diabatic heat fluxes were more with vegetation canopy due to re-emission of longwave radiation by the foliage. A net heat flux of 675 w/m² and 500 w/m² were transported to the atmosphere with and without vegetation canopy respectively.

(*iii*) Due to increased transport of heat with vegetation a higher degree of warming of atmosphere can be expected with increased turbulence and wind speeds. The simulated wind speeds and vertical velocities with vegetation show precisely this. The net warming and subsequent increase in PBL depth show the increase in intensity of turbulence in PBL. The warming is the combined effect of lower foliage albedo and re-emission of longwave radiation by the plant canopy which developed a higher temperature than the surface. The net warming of the atmosphere was found to depend on the amount of vegetation cover and its characteristics (Kar and Ramanathan 1990). The contribution by surface albedo variations was found to be negligible.

(*iv*) With vegetative cover, the depth of the sea breeze developed at the western edge of the island ($x=8$, $y=10$) at selected hours of the simulation period are shown in Fig. 3. The depth of the sea breeze is deduced from this figure by the change in wind direction. For example, at 1600 hours the depth of the sea breeze $\simeq$ 350 m. At 2000 hours the sea breeze retreated from the island and replaced by an easterly flow at lower levels. The maximum intensity of sea breeze $\simeq$ 2 m/sec developed at 1600 hours as shown in Fig. 3. The developed circulations were more intense as shown by the magnitude of vertical velocities. However, the inland penetration distance was found to be less than over a bare soil. This could be due to surface temperature and soil specific humidity differences.

(*v*) Simulated boundary layer velocity profiles at 1400 hours for case 2 and case 3 are shown in Fig. 4. Above plant canopy level (>15 m) higher wind speeds were seen developed with its maximum at about 50 m above the ground. Over bare ground maximum wind speeds were at 20 m above the ground. Higher wind speeds

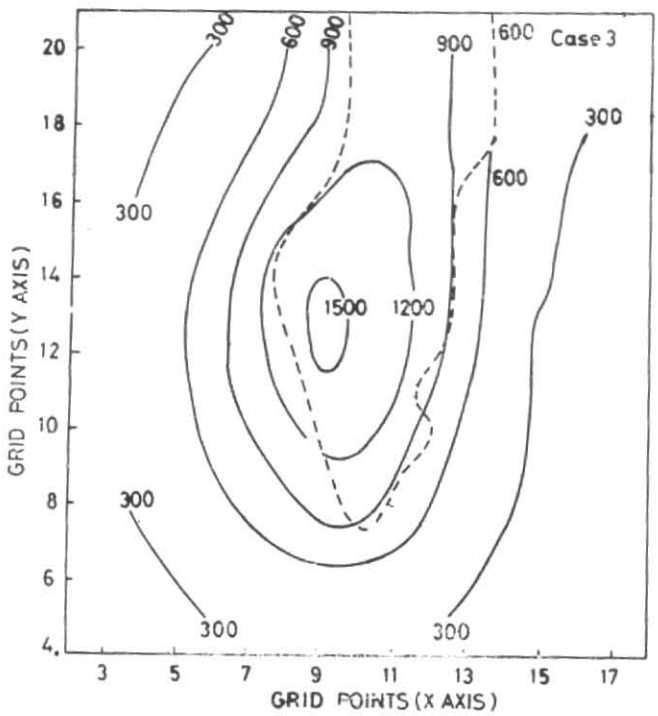

Fig. 5. Height contours of PBL at 1400 IST—case 3

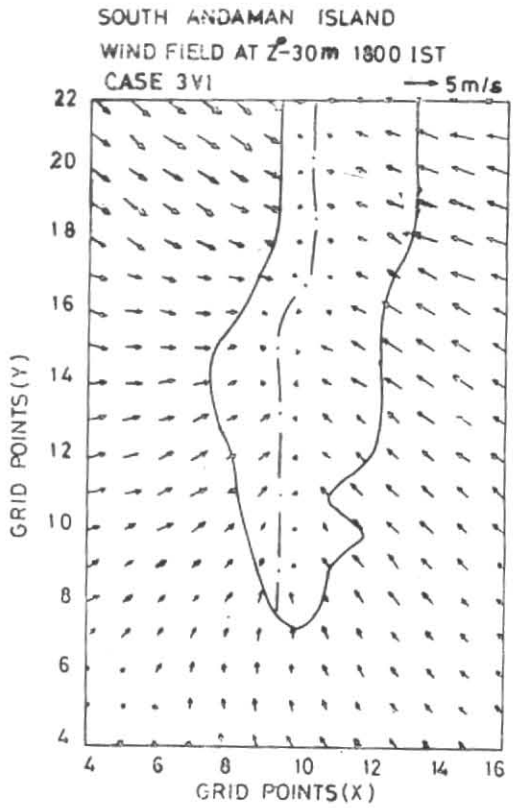

Fig. 6. Simulated wind speeds at 1800 IST, 30 m above ground (case 3). The length of arrow is proportional to wind speed. Sea breeze convergence zone is shown by dash dot across the island

above the plant canopy are due to enhanced turbulence by the canopy are obtained for case 3. The wind speeds are highest during middle of the day with increased turbulence transfer of momentum. Within the canopy wind speed decreases going to zero at the ground (Oke 1978). The simulated profile is in agreement with the above observations. The above results show the vegetation, as secondary source of heat to atmosphere, intensified the developed circulations and modified the characteristics of airflow significantly. Thus, the neglect of ground vegetation cover in atmospheric simulations, could seriously jeopordise the final results.

5.3. *Lateral variations*

The principal difference between 2D and 3D simulations, is 2D simulations assume the homogeneity of all meteorological fields and topography in the meridional direction ($\partial/\partial y=0$) in the entire simulation period. In 3D simulations this restriction is removed so that one includes the spatial variations of these parameters over the whole area (x-y plane). Since the atmospheric flows in nature remain 3 dimensional, the neglect of lateral variations is physically unrealistic. The effect of including the meridional changes are seen from a comparison of 3D model simulated values with the 2D simulation (with topography and vegetation) values tabulated in Table 2 (case 3 and case 4 results).

In 2D simulation we considered a rectangular island with straight coastal geometry extending infinitely along north-south direction. The average width of the island was taken to be 25 km. The terrain height was taken to be the same as in $y=10$ cross-section. Calculations were performed with same set of initial data setting meridional terms to zero at appropriate places in the governing equations.

The tabulated results show that the lower surface temperature with higher soil specific humidity was obtained in 3D simulation. Correspondingly, the developed circulations were less intense compared to 2D model results, as shown by the reduction in magnitudes of vertical velocity, wind speed and boundary layer depth. Since the forcing functions such as topography, initial data are the same, this reduction could be due to advection effects. The 3D simulations had shown that the southerly flow (*i. e.*) from cooler south sea side predominated the northerly flow developed in noon hours as shown in Fig. 6 for 1800 hours. This resulted a reduction in the magnitudes of vertical velocity, surface temperature and increased in the ground specific humidity by reduced evaporation. In short, the developed circulations were less intense. Since in 2D simulations such meridional flows (y directional) are neglected, more intense circulations were simulated. Considerable variations in flow characteristics were also noticed along

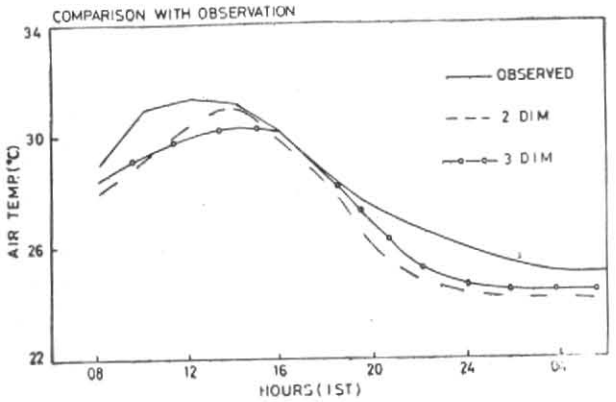

Fig. 7. Comparison of 3D and 2D model predicted temperatures with observations recorded at Port Blair 30 m height

the meridional direction of the island. For example, the results obtained at different cross-sections (y=10 and y=15) are given in Table 3.

The above results show that the island experienced non-uniform surface heating during day. Consequently, the developed circulations close to the centre of island and at y=10 cross-section appeared with different characteristics.

At and near the western edge of the island (y=15, x=9), the land surface temperatures developed more higher than the rest of the island. More heat was transported from this area (=1000 w/m²) as shown in Table 3. Since the change in PBL height is proportional to the surface heat flux ($u_* \theta_*$), the height variations may be taken proportional to heat flux variations. Thus, at the places where PBL height ~600 m the heat flux is approximately half than that found at 1200 m. As the diurnal changes in sea surface temperature were negligible compared to land surface temperature changes, the PBL height varied near the edges of island by advection and diffusion while it remained unchanged near the lateral boundaries. Due to asymmetries in the surface heating and transport of heat flux to the atmosphere the development of PBL over the entire simulated area was not uniform. This is illustrated in Fig. 5.

The model predicted horizontal wind speeds at 1800 hrs, 30 m above the surface is shown in Fig. 6. In this figure the lengths of arrows are drawn proportional to wind speeds and their inclinations mark the wind direction. Weak southerly winds dominated the southern tip of the island. Westerly and northwesterly winds were simulated at the western edge of the island above y=12. The sea breeze convergence zone is shown by a dashed line in the middle of the diagram. At and near the centre of island, it is located at about 15 km from the western edge, while at y=10 the distance is about 4.0 km as given in Table 3. The convergence zones are possible locations for cumulus clouds developments. It can be used for forecasting the occurrence of cumulus activity and thunderstorm developments. Such possibilities were indicated in Findlater (1964) who had shown very close coincidence between the location of thunderstorm centres and convergence zones in England.

TABLE 3

Comparison of magnitudes of flow variables at different cross-sections of island (3D results)

Particulars	y=10	y=15
Temperature difference between east and west end of island	1.5 °C	2.5 °C
Surface specific humidity	33.0 g/kg	31.0 g/kg
Net heat flux	675 w/m²	1000 w/m²
PBL depth at 1400 IST	900 m	1200 m
Sea breeze wind speed	2.3 m/s	4.0 m/s
Vertical velocity at 1200 IST	4.0 cm/sec	12 cm/sec
Horizontal island penetration in km	4.0	15.0

These spatial variations of wind speeds, sea breeze convergence zone and PBL height variations over the island, hitherto not obtained, can be of considerable significance in planning/location of industrial, recreational centres on the island. At night hours, the simulated drainage flow had a depth of about 40 m and was more intense with vegetative cover.

5.4. *Comparison with observations*

Due to paucity of meso-scale network observations in the island, we compare the 3D simulated results with observations at Port Blair. These are shown in Fig. 7. The 3D model predicted temperatures are in good agreement with observations. But, although an improvement was achieved in the prediction of wind field by 3D simulation, the wind field for both the 2D and 3D simulations remained over-estimated. At this level, these deviations could be an outcome of linear interpolation of the Pibal data.

In the absence of dense meso-scale observations in this area it is difficult to evaluate the impact of meso-scale disturbances on the local circulations. However, this study has shown the maximum heat input to the atmosphere by the island is approximately 600-700 w/m². Due to spatial variations of the heat input the PBL heights developed over the island during the day varied considerably. The magnitude of the heat input by the tropical island is in agreement with the observations (Pielke 1984, pp. 399).

6. Conclusions

A three dimensional simulation was made to study the air flow over south Andaman island. We included soil moisture, ground albedo, surface vegetation, coastal and topographic asymmetries in the model. The intensity of the induced perturbations was enhanced by topography and ground vegetation. Further studies will be needed to consider clouds in the radiation balance.

Acknowledgements

The authors gratefully acknowledge Prof. R.A. Pielke for providing a listing of UVMM model. Computations were performed in NEC system of NIC, New Delhi.

References

Abbs, D., 1986, *Mon. Weath. Rev.*, **114**, 831-848.

Clapp, R. and Hornberger, G., 1978, *Water Resour. Res.*, **14**, pp. 601-604.

Coinco, R.M., 1985, *Forest-Atmos. Interaction*, Reidal Publ., pp. 501-521.

Deabreausa, L. *et al.*, 1988, *J. Theor. Appl. Cli.* (Preprint copy).

Deardorff, J.W., 1978, *J. geophy. Res.*, **83**, 1889-1903.

Findlater, J., 1964, *Met. Mag.*, **93**, 82-89.

Garrett, A. J., 1983, *J. Cli. and appl. Met.*, **23**, 79-90.

Idso, S.B., Jackson, R.D., Reginato, R.J., Kimball, B.A. & Nakayama, F.S., 1975, *J. appl. Met.*, **14**, pp. 109-113.

Jager, L., 1985, *Forest-Atmos. Interaction*, Reidal Publ., pp. 59-71.

Kar, S.C. and Ramanathan, N., 1987, *Proc. Ind. Acad. Sci.*, **96**, pp. 169-188.

Kar, S.C. and Ramanathan, N., 1989, *Proc. Ind. Nat. Sci. Acad.*, **55**, A, pp. 871-885.

Kar, S.C. and Ramanathan, N., 1990, *Mausam*, **41**, 81-88.

Kumar, A. and Barathakur, N., 1971, *Bound. Lay. Met.*, **2**, 218-227.

Lee, R., 1978, Forest Micro Met., Columbia Univ. Press, pp. 87.

Mahrer, Y. and Pielke, R.A., 1976, *Mon. Weath. Rev.*, **104**, 1392-1402.

Mahrer, Y. and Pielke, R.A., 1977, *Contrib. Atmos. Phys.*, **50**, 93-113.

Mccumber, M.C., 1980, Ph.D. Thesis, University of Viriginia.

Mccumber, M.C. and Pielke, R.A., 1981, *J. Geophys. Res.*, **86**, 9929-9938.

Monteith, J.L., 1973, Principles of Environmental Physics, Edwin Arnold Pub., 241 pp.

Neumann, J. and Mahrer, Y., 1974, *J. Atmos. Sci.*, **31**, 2027-2039.

Nickerson, E.C., 1979, *Contrib. Atmos. Phys.*, **53**, 161-175.

Oke, T.R., 1978, *Boundary Layer Climates*, Methuen and Co., 372 pp.

Ookouchi, Y. and Wakata, Y., 1984, *J. met. Soc. Japan*, **62**, 864-879

Perrier, A., 1978, *Land Surface Processes : Vegetaion* (Ed) P.S. Eagleson, Camb. Univ. Press, 395-448.

Pielke, R.A., 1984, *Meso-scale Meteorological Modelling*, Acad. Press, 377-418.

Simpson, J., 1985, *Forest-Atmos. Interaction*, Reidal Publ., pp. 197.

Stanhill, 1969, *J. appl. Met.*, **8**, 509-513.

Segal, M., Mahrer, Y. and Pielke, R.A., 1982, *J. appl. Met.*, **21**, 1754-1762.

Thom, A.S., 1971, *Quart. J. Roy. met. Soc.*, **97**, pp. 414-428.

Yamada, T., 1982, *J. met. Soc. Japan*, **60**, 439-454.